Available online at www.sciencedirect.com
ScienceDirect
Nuclear Medicine and Biology 36 (2009) 711–719
NUCLEAR MEDICINE — AND — BIOLOGY
www.elsevier.com/locate/nucmedbio

Reproducibility of the kinetic analysis of 3′-deoxy-3′-[^{18}F] fluorothymidine positron emission tomography in mouse tumor models

Seung Jin Choi[a], Seog Young Kim[a], Su Jin Kim[b], Jae Sung Lee[b], Sang Ju Lee[c], Soo Ah Park[d], Seung Jin Lee[d,e], Sung-Cheol Yun[f], Ki Chun Im[a], Seung Jun Oh[a,d], Sang-We Kim[g], Jae Seung Kim[a,d], Jin Sook Ryu[a,d], Dae Hyuk Moon[a,d,e,*]

[a]*Department of Nuclear Medicine, Asan Medical Center, University of Ulsan College of Medicine, Seoul, South Korea*
[b]*Department of Nuclear Medicine, Seoul National University College of Medicine, Seoul, South Korea*
[c]*Department of Chemistry, Sogang University, Seoul, South Korea*
[d]*Molecular Imaging Center, Asan Institute for Life Sciences, Asan Medical Center, Seoul, South Korea*
[e]*Institute for Innovative Cancer Research, Asan Medical Center, Seoul, South Korea*
[f]*Department of Preventive Medicine, Center for Medical Research and Information, University of Ulsan College of Medicine, Seoul, South Korea*
[g]*Division of Oncology, Department of Internal Medicine, Asan Medical Center, University of Ulsan College of Medicine, Seoul, South Korea*

Received 15 December 2008; received in revised form 27 March 2009; accepted 14 June 2009

Abstract

Objectives: We assessed the reproducibility of the kinetic analysis of 3′-deoxy-3′-[^{18}F]fluorothymidine (FLT) positron emission tomography (PET) in A431 human epidermoid carcinoma and murine Lewis lung carcinoma (LLC) tumor models.
Methods: We injected 7.4 MBq of FLT (n=10 for each group) and acquired 2-h dynamic PET images. A second scan was performed 1 day later. We calculated standardized uptake value (SUV), kinetic rate constants, volume of distribution of phosphorylated FLT (V_{dm}), net influx constant ($K_{FLT\text{-}CA}$) and influx constant by Patlak graphical analysis ($K_{FLT\text{-}PA}$). The percent difference between measurements of a parameter was calculated to compare the reproducibilities of different parameters.
Results: FLT phosphorylation was higher in mice with A431 tumors than in mice with LLC tumors (P<.005). Differences in the standard deviations of the percent differences of parameters were statistically significant (P<.001) in each model. In mice with A431 tumors, SUV, V_{dm}, $K_{FLT\text{-}CA}$ and $K_{FLT\text{-}PA}$ had standard deviations of the percent difference of ≤20%. The most reproducible parameter was $K_{FLT\text{-}PA}$, although the standard deviation (15.6%) was not statistically different from those of V_{dm} (15.8%), $K_{FLT\text{-}CA}$ (17.5%) and SUV (18.9%). In mice with LLC tumors, K_1, K_1/k_2 and k_3 had standard deviations of the percent difference of ≤20%. No macroparameters reflecting a total FLT flux had standard deviations of ≤20%.
Conclusion: Our results show the reproducibility of the kinetic macroparameters of FLT PET in mouse tumors with high FLT phosphorylation.

Keywords: Reproducibility; 3′-Deoxy-3′-[^{18}F]fluorothymidine; Positron emission tomography; Kinetic analysis; Mouse

1. Introduction

Current standards for monitoring anticancer treatments are defined by the treatment-induced reduction of tumor size [1]. However, measurement criteria are not universally applicable to all tumor types and drug classes [2,3]. In addition, it often takes considerable time before a tumor becomes measurably smaller, and scar tissue or edema may mask tumor regression [4]. Molecular imaging that measures the proliferative activity of tumors may give an important insight into the assessment of anticancer treatment response because proliferative activity is a hallmark of malignant tumors and has significant prognostic and predictive importance [5]. Positron emission tomography (PET) with 3′-deoxy-3′-[^{18}F]fluorothymidine (FLT) reflects cellular proliferation by measuring thymidine kinase 1 activity [6].

* Corresponding author. Department of Nuclear Medicine, Asan Medical Center, University of Ulsan College of Medicine, Seoul 138-736, South Korea. Tel.: +82 2 3010 4592; fax: +82 2 3010 4588.
E-mail addresses: dhmoon@amc.seoul.kr, daehyukmoon@hanmail.net (D.H. Moon).

0969-8051/$ – see front matter © 2009 Elsevier Inc. All rights reserved.
doi:10.1016/j.nucmedbio.2009.06.001

Preclinical and clinical studies have shown the potential of FLT PET in the assessment of responses to therapy, especially early in the course of treatment [7–15].

The in vivo changes following anticancer treatment are complex and result in different tumor protein expression profiles [16,17]. In addition, anticancer therapy can cause changes in perfusion and in the physiological biodistribution of FLT [7]. Therefore, changes in the expression and function of proteins and enzymes that are important for thymidine metabolism following anticancer therapy and their effects on FLT metabolism must be elucidated before FLT metabolism can be adopted as an imaging biomarker for the assessment of treatment response [18]. Kinetic modeling of FLT using compartmental analysis can accurately determine FLT delivery, phosphorylation and dephosphorylation independent of scanning time or alterations in plasma clearance following therapy [19–23]. Moreover, FLT kinetic parameter correlates better with Ki-67 labeling index than does standardized uptake value (SUV) [20,24]. Complexity in data acquisition and the need for arterial sampling are no longer issues in FLT kinetic imaging because there is no spillover from myocardial activity, no partitioning between whole blood and plasma, negligible protein binding and no difference in the metabolites of arterial and venous samplings [19,21,23]. Furthermore, because there are no FLT metabolites in mice plasma, left ventricular activity can be used as an image-derived input function without any need to sample arterial or venous plasma [7,23].

The main limitation of compartmental kinetic analysis is that variability in parameters may not allow reliable data interpretation or detection of treatment-induced changes. With the increasing use of animal PET imaging studies in assessing therapy response and preclinical drug screening, the reproducibility of data must be well documented [25]. However, the reproducibility of FLT PET imaging has been evaluated only for the static parameters of FLT uptake [13,26]. We have previously described a three-compartment four-rate constant model for FLT in two tumor mouse models with different FLT kinetics [23]. The aim of this study was to assess the reproducibility of FLT dynamic PET data acquired in two mouse tumor models. We also intended to compare the reproducibilities of kinetic and static parameters in test–retest studies.

2. Methods

2.1. Radiopharmaceutical preparation

FLT was prepared by nucleophilic fluorination of [^{18}F] fluoride and 5′-*O*-DMTr-2′-deoxy-3′-*O*-nosyl-β-D-threo-pentafuranosyl)-3-*N*-BOC-thymine as precursors in a protic solvent (*t*-butanol or *t*-amyl alcohol) [27]. Typical decay-corrected radiochemical yields were 60–70%, the radiochemical purity was 98±1.2% after high-performance liquid chromatography purification and the specific activity was 75.5±4.1 TBq/mmol (range: 68.0–82.5 TBq/mmol) at the time of injection. The amount of FLT injected was 98.3±5.3 pmol (range: 89.7–108.7 pmol).

2.2. Cell lines

A431 human epidermoid carcinoma and murine Lewis lung carcinoma (LLC) cell lines were obtained from the American Type Culture Collection (Manassas, VA). Cells were routinely cultured in Dulbecco's/Vogt-modified Eagle's minimal essential medium supplemented with 10% (vol/vol) heat-inactivated fetal bovine serum, L-glutamine (2 mM), penicillin (100 IU/ml) and streptomycin (50 μg/ml) (Gibco Invitrogen Corporation, Carlsbad, CA). The cells were maintained at 37°C in air with 5% (vol/vol) CO_2.

2.3. Mouse tumor models

To create tumor models, we used 6-week-old male Balb-c/nu mice (A431 human carcinoma) and C57BL/6 mice (murine LLC). These mice were purchased from Charles River Laboratories (SLC, Japan). The research protocol was approved by the Institutional Animal Care and Use Committee of the Asan Institute for Life Science, and mice were maintained in accordance with the Institutional Animal Care and Use Committee guidelines of the Asan Institute for Life Science. Exponentially growing cells (7×10^6 A431 cells or 1×10^6 LLC cells) suspended in 200 μl of culture medium were injected subcutaneously into the right forelimbs of anesthetized mice. Tumor sizes were continuously measured using calipers, and volumes were calculated using the equation: volume=$(\pi/6)abc$, where a, b and c represent the three orthogonal axes of the tumor, respectively. When the mean tumor diameter was 5–7 mm, the mice were used for imaging experiments. Our previous study has shown significantly different levels of thymidine kinase activity and percent Ki-67 between A431 and LLC tumors [23]. The experiments were carried out in compliance with Korean laws relating to the conduct of animal experimentation.

2.4. PET imaging

A commercially available PET system (Focus 120 microPET; Siemens, Knoxville, TN) was used for imaging [28]. Fours hours prior to imaging, mice were deprived of food, and both tumor size and body weight were recorded. Two-hour dynamic PET scans were acquired after a tail vein injection of 7.4 MBq (0.2 mCi) of FLT. All intravenous injections were successful. The dynamic imaging sequence was 4×3, 6×1, 7×6, 8×30, 1×300 and 11×600 s, with 128×128×95 matrices and a voxel size of 0.432×0.432×0.796 mm^3 [23]. Mice were maintained under isoflurane anesthesia during the entire procedure. To assess reproducibility, we performed a second PET scan 1 day later, after the reinjection of 7.4 MBq of FLT.

Three mice were excluded from the study due to acquisition failure (n=2) and acquisition with erroneous

parameters (n=1). Finally, 10 mice with A431 tumors and 10 mice with LLC tumors were analyzed. PET images were reconstructed by filtered backprojection using a Hamming filter with a cutoff frequency of 0.5 cycle/pixel. No attenuation correction was applied. The modes of data acquisition and reconstruction were identical for the test and retest PET scans.

2.5. PET image analysis

Volumes of interest (VOI) were applied to the dynamic image set for data extraction, as described previously [23]. For the left ventricular cavity, a seven-pixel circular region of interest was centered on the location of the maximum pixel value in the initial dynamic images (Fig. 1A). The left ventricular time–activity curve was corrected for partial-volume effect by using a recovery coefficient of 0.924 [23].

The last frame of the dynamic acquisition was used to define VOI for the analysis of FLT activity in A431 (Fig. 1B) and LLC (Fig. 1C) tumors. Tumor VOI were constructed by creating a seven-pixel circular region of interest from three consecutive slices centered on the location of the maximum pixel value of tumor regions [23]. The percent injected dose per gram of tumor tissue (%ID/g) and the SUV of the tumor were calculated from the last frame of the dynamic study (110 min after injection).

A three-compartment model with five parameters was used to analyze the dynamic FLT PET data, as previously described [19] (Fig. 2). In our previous study, we established a kinetic modeling analysis method for quantitative FLT PET studies in these subcutaneous tumor models [23]. The regional VOI–activity curves and blood time–activity curves were fitted by the FLT compartmental model using the weighted Levenberg–Marquart least-squares minimization algorithm, as implemented in a software package designed for the analysis of PET data (PMOD version 2.65; PMOD Group, Zurich, Switzerland). The five parameters were K_1, V_d ($=K_1/k_2$), k_3, k_4 and the fraction of vascular space in the tissue. V_d estimates the early distribution volume of FLT in tumor tissues. The initial values for these parameters were set to 0.1, 1.0, 0.1, 0.01 and 0.05 for A431 and to 0.1, 0.5, 0.01,

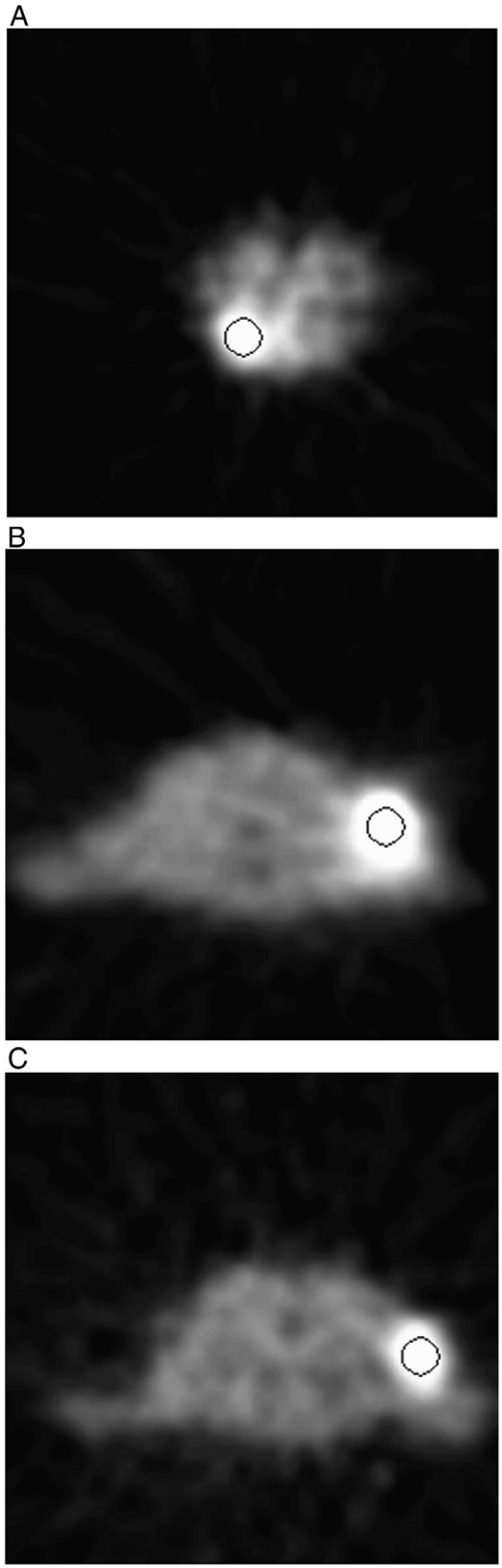

Fig. 1. Typical transaxial images of mice with A431 or LLC tumors after intravenous administration of 7.4 MBq of FLT. Mice were maintained under isoflurane anesthesia during the entire procedure. (A) Early dynamic image of FLT showing left ventricular activity. A seven-pixel circular region of interest centered on the location of maximum pixel value and three consecutive axial slices were combined to create a cylindrical VOI to measure left ventricular input function. (B) Transaxial image in a Balb-c/nu mouse with A431 human carcinoma obtained 110 min after a bolus injection of FLT, showing high activity in the tumor. A seven-pixel circular region of interest drawn in the center was used to generate a tumor time–activity curve. (C) Transaxial slice of a 110- to 120-min-postinjection FLT image of a C57BL/6 mouse with LLC. The FLT activity within the region of interest is lower than that seen in A431 mice (B).

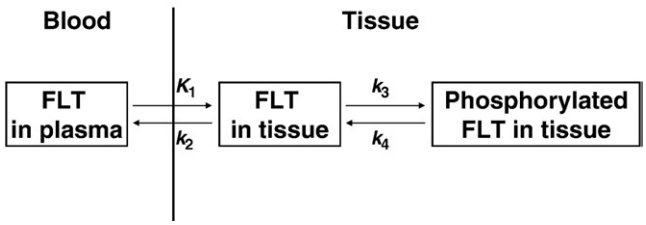

Fig. 2. Three-compartment FLT model with four rate constants used to describe transport and metabolism between compartments. The model has an exchangeable tissue compartment and a compartment of trapped FLT phosphate nucleotides. K_1 and k_2 are rate constants for the forward transport and reverse transport of FLT between plasma and tissue, respectively. The rate constants between the precursor and the phosphorylated FLT denote the thymidine-kinase-mediated phosphorylation (k_3) and dephosphorylation (k_4) of FLT.

0.01 and 0.05 for LLC, respectively. Then, the net influx constant ($K_{\text{FLT-CA}}$) and the volume of distribution of phosphorylated FLT (V_{dm}) were calculated as follows:

$$K_{\text{FLT-CA}} = \frac{K_1 k_3}{K_1/V_{\text{d}} + k_3}$$

$$V\text{dm} = V_{\text{d}} \frac{k_3}{k_4}$$

Patlak graphical analysis was also performed with the same software package to calculate the FLT blood–tissue transfer constant (the net influx constant $K_{\text{FLT-PA}}$). A regression slope was obtained by fitting a regression line within 30–70 min. This time interval was chosen after an examination of the linearity of different tumor regions.

2.6. Calculation of reproducibility and statistical analysis

One experienced investigator drew VOI on the first FLT PET images and calculated all static and dynamic parameters. Then, the same investigator analyzed the same initial PET images repeatedly at least 1 week later for assessment of intraobserver reproducibility. For assessing interobserver reproducibility, the second investigator analyzed the first FLT PET images. For test–retest reproducibility, the first investigator recalculated all parameters of the retest PET images without information on their identity or on values of previously calculated parameters.

The mean and the standard deviation of the difference between measurements of a parameter d were calculated to assess intratest, intertest and test–retest reproducibilities. Percent difference D (d divided by the mean of two measurements) was also calculated to compare the reproducibilities of different parameters. The differences in parameters between the first test and the second test were analyzed with paired t test. The difference in parameters between mice with A431 tumors and mice with LLC tumors was assessed by Student's t test. The homogeneous variance of D in dynamic and static PET parameters was analyzed by the likelihood ratio test, using random-effects models. Intraclass correlation coefficients (ICCs) that describe reproducibility and the correlation between two measurements of a parameter were determined by random-effects models.

Statistical analyses were performed with the Statistical Package for the Social Sciences for Windows (SPSS 12.0KO for Windows release 12.0.1; SPSS, Inc., Chicago, IL) and the Statistical Analysis System program version 9.1

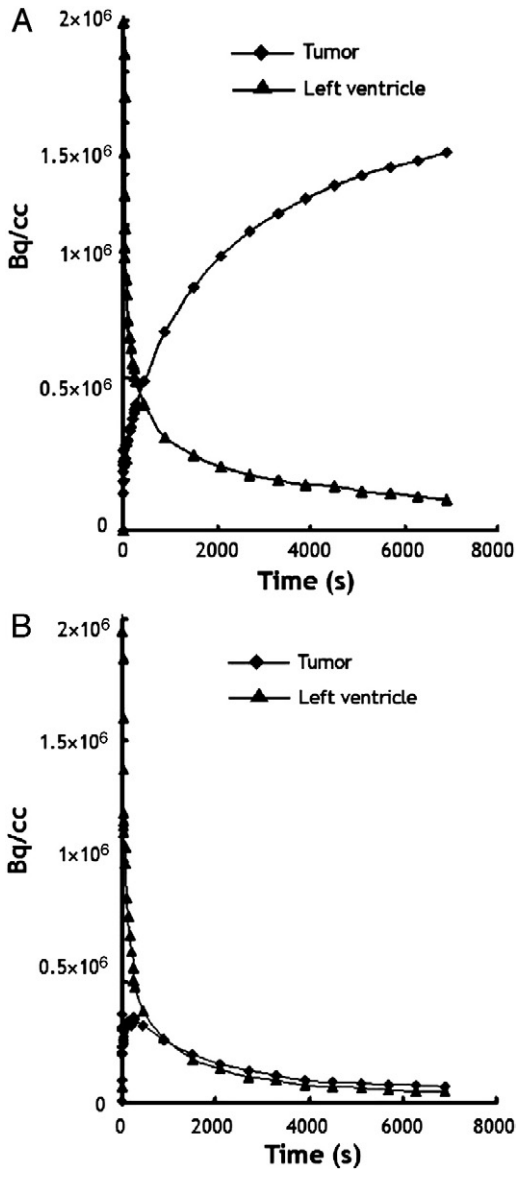

Fig. 3. Representative decay-corrected time–activity curves of FLT uptake in the left ventricle and tumor of a Balb-c/nu mouse bearing A431 human carcinoma (A) and of a C57BL/6 mouse with LLC tumor (B). An image-derived left ventricular time–activity curve and a tumor time–activity curve were fitted by the three-compartmental model to estimate kinetic parameters. Patlak graphical analysis was also performed to estimate the FLT blood–tumor transfer constant using these tumor and blood time–activity curves. Mice with the A431 tumor (A) accumulated FLT with time, but mice with the LLC tumor (B) did not.

(SAS Institute, Cary, NC). $P<.05$ was considered statistically significant.

3. Results

3.1. Mouse tumors and dynamic FLT PET imaging

The average body weights of mice with A431 and LLC tumors on the day of the initial FLT PET study were 23.8±1.2 and 24.2±1.1 g, respectively. These were not significantly different from the average body weights on the day of retest PET (23.7±1.4 and 24.2±1.3 g). However, the average tumor volumes (A431, 77.1±23.6 mm^3; LLC, 104.8±40.0 mm^3) were significantly greater on the day of the retest PET (A431=113.0±33.9 mm^3, $P<.005$; LLC=138.7±46.1 mm^3, $P<.005$).

Fig. 3 shows representative left ventricular and tumoral time–activity curves of FLT. After intravenous injection, there was an initial rapid decline in left ventricular FLT activity, and this was followed by a slow decline in A431 and LLC tumors. Dynamic studies of mice with A431 tumors indicated a continuous accumulation of FLT in the tumor tissue over the entire 2-h measurement period (Fig. 3A). In contrast, those with LLC tumors showed a low level of FLT retention (Fig. 3B).

3.2. Intraobserver and interobserver reproducibilities

Measurements of the same FLT PET dynamic images performed to assess intraobserver (two analyses, one observer) and interobserver (two observers) reproducibilities showed no significant differences in parameters. The standard deviation of the percent difference was 1.6–16.8%, with an ICC of 0.84–1.00 for intraobserver variability (Table 1). There were significant differences in the standard deviation of the percent difference between parameters ($P<.001$). In both types of tumors, static parameters (SUV and %ID/g) had higher reproducibility than microkinetic parameters, as indicated by the low standard deviation of the percent difference (3.3% for A431 and 1.6% for LLC) and a high ICC of 1.0. Kinetic macroparameters (A431: V_{dm}, $K_{FLT\text{-}CA}$ and $K_{FLT\text{-}PA}$; LLC: K_1/k_2, V_{dm} and $K_{FLT\text{-}CA}$) also showed comparable intraobserver reproducibility.

Analysis of interobserver reproducibility showed that the standard deviation of the percent difference was 0.9–13.5%, with an ICC of >0.95 (Table 2). The standard deviation of the percent difference also varied significantly between parameters ($P<.001$). As in the case of intraobserver variability, static parameters (SUV and %ID/g) and macroparameters (A431: V_{dm}, $K_{FLT\text{-}CA}$ and $K_{FLT\text{-}PA}$; LLC: V_{dm}) had high interobserver reproducibility.

3.3. Test–retest reproducibility

Table 3 shows the means and standard deviations of the measured parameters from the first and second studies with differences and percent differences. There were significant differences in several kinetic and static parameters between mice with A431 tumors and mice with LLC tumors ($P<.005$). Parameters that reflect FLT transport and phosphorylation (K_1/k_2, k_3, V_{dm}, $K_{FLT\text{-}CA}$, $K_{FLT\text{-}PA}$, SUV and %ID/g) were higher in mice with A431 tumors than in mice with LLC tumors. However, k_4 was lower in mice with A431 tumors. There were no significant differences in the other parameters.

There were no significant differences in parameters between the first scan and the second scan of mice with A431 tumors. However, in mice with LLC tumors, there were significant differences in k_4, V_{dm} and $K_{FLT\text{-}PA}$ ($P<.05$) (Table 3).

The standard deviation of the percent difference between serial FLT PETs in A431 tumors ranged from 15.6%

Table 1
Intraobserver reproducibility

Parameter	A431 (n=10)			LLC (n=10)		
	d	D^a (%)	ICC	d	D^a (%)	ICC
K_1	0.015±0.074	4.4±16.8	0.84	0.003±0.014	1.6±7.6	0.94
K_1/k_2	−0.071±0.144	−6.8±15.8	0.97	−0.003±0.011	−0.9±2.1	0.97
k_3	0.013±0.025	9.4±12.3	1.00	0.000±0.001	2.4±6.2	0.99
k_4	0.000±0.001	3.4±5.1	0.98	0.000±0.001	2.1±4.3	1.00
V_{dm}	0.122±0.630	−0.9±4.4	1.00	−0.007±0.017	−0.6±2.9	1.00
$K_{FLT\text{-}CA}$	0.001±0.004	2.5±5.7	0.99	0.000±0.000	1.5±4.5	0.99
$K_{FLT\text{-}PA}$	0.000±0.001	0.5±4.3	1.00	0.000±0.000	−2.4±8.4	1.00
SUV	0.047±0.083	1.2±3.3	1.00	−0.001±0.005	−0.1±1.6	1.00
%ID/g	0.203±0.349	1.2±3.3	1.00	−0.002±0.020	−0.1±1.6	1.00

Difference and percent difference of the calculated parameters of FLT PET in mice with A431 and LLC tumors, as measured by repeated analysis by a single investigator.

d, difference between measurements of a parameter; D, percent difference (d divided by the mean of two measurements); K_1, k_2, k_3 and k_4, rate constants describing the kinetic transfer rates of FLT or phosphorylated FLT between two compartments; V_{dm}, volume of distribution of phosphorylated FLT; $K_{FLT\text{-}CA}$, the net influx constant of FLT determined by compartmental analysis; $K_{FLT\text{-}PA}$, the net influx constant determined by Patlak graphical analysis; %ID/g, percent injected dose per gram of tumor tissue.

[a] Difference in the standard deviation of the percent difference between parameters in each tumor model ($P<.001$).

Table 2
Interobserver reproducibility

Parameter	A431 (n=10)			LLC (n=10)		
	d	D^a (%)	ICC	d	D^a (%)	ICC
K_1	0.007±0.028	1.1±9.5	0.95	−0.000±0.013	−0.0±6.0	0.96
K_1/k_2	−0.010±0.076	−1.4±6.9	0.99	−0.002±0.019	−0.4±3.0	0.96
k_3	0.004±0.014	−0.3±9.4	1.00	0.000±0.002	1.8±13.5	0.87
k_4	−0.000±0.000	−2.6±4.1	0.99	0.000±0.002	1.2±9.6	0.99
V_{dm}	0.232±0.606	0.9±2.6	1.00	0.004±0.017	0.2±3.8	1.00
$K_{FLT\text{-}CA}$	−0.000±0.004	−0.7±5.1	0.99	0.000±0.001	1.3±10.8	0.93
$K_{FLT\text{-}PA}$	0.000±0.002	0.0±3.7	1.00	0.000±0.000	−2.0±11.4	1.00
SUV	−0.024±0.070	−0.8±2.1	1.00	−0.000±0.003	−0.1±0.9	1.00
%ID/g	−0.101±0.292	−0.8±2.1	1.00	−0.001±0.012	−0.1±0.9	1.00

Difference and percent difference of the calculated parameters of FLT PET in mice with A431 and LLC tumors, as determined from the analysis by two investigators.

[a] Difference of the standard deviation of the percent difference between parameters in each tumor model (P<.001).

($K_{FLT\text{-}PA}$) to 41.3% (K_1); this difference was significant (P<.001). ICCs ranged from 0.24 (K_1) to 0.99 (V_{dm}) (Table 3). Only static parameters (SUV and %ID/g) and macroparameters (V_{dm}, $K_{FLT\text{-}CA}$ and $K_{FLT\text{-}PA}$) had standard deviations of ≤20%. The most reproducible parameter was $K_{FLT\text{-}PA}$, although the standard deviation was not statistically different from those of V_{dm}, $K_{FLT\text{-}CA}$, SUV and %ID/g.

In mice with LLC tumors, K_1, K_1/k_2 and k_3 had standard deviations of the percent difference of ≤20%, with ICC values ranging from 0.51 to 0.70 (Table 3). The difference in standard deviations between parameters was also statistically significant (P<.001). The standard deviation of the percent difference of the most reproducible parameter (K_1/k_2=8.6%) was similar to those of K_1, k_3, $K_{FLT\text{-}CA}$ and %ID/g, but significantly different from that of SUV (P<.05).

4. Discussion

Our study on the test–retest reproducibility of the kinetic analysis of FLT PET in mouse tumor models showed that the measurement of static and macrokinetic parameters was reproducible (standard deviation of ≤20%) in A431 tumors that had a high phosphorylation of FLT. Static parameters and macroparameters that reflect FLT transport and phosphorylation (V_{dm}, $K_{FLT\text{-}CA}$ and $K_{FLT\text{-}PA}$) were the most reproducible. In LLC tumors that had a low phosphorylation of FLT, however, K_1, K_1/k_2 and k_3 were reproducible, whereas other static and kinetic parameters showed poor reproducibility. The most reproducible parameter was the initial volume of distribution of free FLT (K_1/k_2), which was even more reproducible than that of SUV.

Table 3
Test and retest reproducibility of the kinetic parameters of FLT PET in mice with A431 and LLC tumors

Parameter		Test	Retest	d	D^a (%)	ICC
A431 (n=10)	K_1	0.204±0.099	0.208±0.082	0.005±0.112	5.1±41.3	0.24
	K_1/k_2	1.124±0.597	1.241±0.581	0.117±0.474	10.1±35.1	0.68
	k_3	0.165±0.240	0.216±0.419	0.052±0.185	7.8±40.6	0.85
	k_4	0.011±0.003	0.012±0.003	0.001±0.002	8.1±21.4	0.81
	V_{dm}	12.292±12.565	13.248±12.954	0.956±1.567	10.2±15.8	0.99
	$K_{FLT\text{-}CA}$	0.069±0.032	0.075±0.031	0.007±0.015	11.7±17.5	0.90
	$K_{FLT\text{-}PA}$	0.047±0.029	0.050±0.025	0.003±0.008	9.3±15.6	0.96
	SUV	3.938±2.467	4.164±2.190	0.226±0.676	9.8±18.9	0.96
	%ID/g	17.015±11.998	18.034±10.830	1.020±2.976	10.1±19.7	0.97
LLC (n=10)	K_1	0.196±0.042	0.206±0.042	0.010±0.033	5.2±17.4	0.70
	K_1/k_2	0.646±0.061	0.667±0.050	0.019±0.055	3.0±8.6	0.51
	k_3	0.017±0.004	0.017±0.004	−0.000±0.003	−0.7±16.7	0.61
	k_4*	0.020±0.011	0.013±0.002	−0.007±0.009	−34.1±32.7	0.19
	V_{dm}*	0.639±0.270	0.904±0.321	0.267±0.294	36.4±38.2	0.51
	$K_{FLT\text{-}CA}$	0.011±0.002	0.011±0.003	0.000±0.002	2.4±20.2	0.51
	$K_{FLT\text{-}PA}$*	0.003±0.002	0.005±0.002	0.002±0.002	51.2±59.4	0.50
	SUV	0.294±0.093	0.312±0.061	0.019±0.101	8.1±29.7	0.17
	%ID/g	1.224±0.418	1.289±0.243	0.066±0.411	7.9±28.6	0.28

Differences in k_4, V_{dm}, $K_{FLT\text{-}CA}$, $K_{FLT\text{-}PA}$, SUV and %ID/g between A431 and LLC tumors (P<.005).

[a] Difference in the standard deviation of the percent difference between parameters in each tumor model (P<.001).

* P<.05 between test and retest parameters.

Our estimates of $K_{FLT\text{-}CA}$ with a standard deviation of the percent difference of 17.5% in A431 tumors indicate that a change in the net FLT influx of more than 35% (twice the percent difference) predicts actual changes in tumors. On the other hand, in LLC tumors, the standard deviation of the percent difference of $K_{FLT\text{-}CA}$ was 20.2%, and none of the macroparameters reflecting a total FLT flux had a standard deviation of the percent difference of ≤20%. Our results indicate that we can potentially detect specific changes in FLT metabolism following anticancer therapy in mice by using FLT PET kinetic parameters, especially in tumors with high FLT phosphorylation.

The high reproducibility of static parameters in intraobserver and interobserver studies can be easily explained by the placement of only one VOI in the tumor. The test–retest reproducibility of the static parameter in this study was also high, but slightly lower than that reported previously for FLT and [^{18}F]fluorodeoxyglucose measurements in mice xenograft models [26,29], and for FLT [13] or [^{18}F]fluorodeoxyglucose measurements in humans [30,31]. We carefully controlled for factors that may have affected reproducibility, such as temperature and size VOI. In addition, we analyzed mice that had 5- to 7-mm-diameter tumors to avoid complications that may be introduced by large tumors, such as necrosis-related heterogeneity [23]. A lower reproducibility of static parameters in our study may be due to our use of different methods and different experimental models. We analyzed images 2 h after injection; the time interval between the two imaging sessions was 24 h. Paravenous FLT injection may also have contributed to the low reproducibility of static parameters in our study. We did not assess the infiltration of the radiotracer in the tail because mice tails were not in the field of view during dynamic PET scans. Subtraction of tail vein activity from the injected dose may improve the reproducibility of static parameters [26]. The lower reproducibility of static parameters in our study may also be due to the variability associated with anesthesia and a spontaneous change in FLT metabolism over 24 h.

The reproducibility of Patlak kinetic analysis in mice with A431 tumors was high and similar to the standard deviation of the percent difference seen in a recent study of patients with breast cancer [13]. However, as expected, in mice with LLC tumors and low FLT uptake, Patlak analysis was not reproducible. As demonstrated in several previous studies, our results also significantly underestimated the net influx of FLT because we ignored k_4 in Patlak kinetic analysis [20,22,23,32,33]. Patlak analysis may not be applied in FLT kinetic analysis in our tumor models due to underestimation of FLT flux.

Our compartmental kinetic analysis showed that kinetic parameters afforded a test–retest reproducibility comparable to static parameters. The reproducibility of our estimation of kinetic parameters may be due to the inclusion of a time–activity curve for input function, rather than the use of injected dose to normalize tumor activity. The amount of FLT that is available for uptake by the tumor is accurately measured without the problems associated with paravenous FLT injection that have contributed to the low reproducibility of static parameters. However, previous dynamic studies with [^{18}F]fluorodeoxyglucose in humans showed that compartmental modeling and Patlak analysis did not improve reproducibility [30,31]. In contrast to [^{18}F]fluorodeoxyglucose studies in humans, we were able to sample a continuous input function from a left ventricular time–activity curve analysis without motion artifacts or spillover activity from the myocardium [23]. Another reason for our better reproducibility in mouse tumor models may be that we had less Poisson noise in radioactivity measurements due to a higher injected dose per weight and the use of a more sensitive PET scanner.

Compared with our estimation of macroparameters that reflect a total FLT flux, our calculations of parameters that reflect either transport or metabolism had poor reproducibility in the A431 model, as shown in previous studies [19,30]. A high level of covariance between transport and metabolism parameters in A431 tumors indicates difficulty in the robust estimation of these microparameters [23]. Instead, errors in estimating microparameters or macroparameters that reflect either transport or metabolism tend to mutually cancel; thus, a total FLT flux, as determined from Patlak graphical analysis or macrokinetic parameters calculated from individual rate constants, has better reproducibility [19]. Previous studies have also shown a high covariance between K_1/k_2 and k_3 in humans [19,32]; thus, a robust estimation of these microparameters may be difficult. In case of LLC tumors that have low FLT phosphorylation, static and kinetic macroparameters that reflect FLT metabolism had poor reproducibility. Instead, the standard deviation of K_1/k_2 was the most reproducible, even significantly different from that of SUV. The results of test–retest reproducibility in LLC tumors may be related to high FLT transport but low phosphorylation.

The high reproducibility of kinetic parameters in tumors indicates that FLT PET imaging can reliably detect anticancer-related changes in these tumors. However, a measurable change in an FLT parameter does not necessarily imply that a treatment-related effect is beneficial. In addition, the kinetics of FLT may differ from that of thymidine [34]. Future studies that employ a large number of subjects, explore different types of tumors and consider different treatment regimens will be required to assess changes following anticancer therapy and to determine whether changes in FLT kinetic parameters reflect treatment efficacy.

In previous reproducibility studies in mice, the second measurement was performed 6 h after the first injection, and researchers assumed that tumor xenografts did not change significantly between the two measurements [26,29]. We performed the second FLT PET measurement 24 h after the first measurement. The initial tumor volume of mice with A431 tumors and mice with LLC tumors

increased significantly on the day of the second PET measurement, and some kinetic parameters showed significant changes in mice with LLC tumors. Therefore, systemic error may exist between two FLT PET measurements. However, we focused on random errors only. We analyzed only standard deviations of differences or percent differences and chose a two-way random-effects model to calculate ICC. The presence of real changes between two studies (systemic errors) does not affect the main results of our study. Furthermore, the differences in all parameters in A431 tumors and in K_1, K_1/k_2, k_3, $K_{FLT\text{-}CA}$ and SUV in LLC tumors between test and retest studies were not significantly different. For the same reason, a possible systemic error between two studies with respect to a partial-volume effect generated by an increase in diameter (11.8% in A431 and 9.8% in LLC) may not affect the result of this study. In this study, partial-volume correction of tumor activity was not performed, considering the resolution of the PET scanner and the size of VOI as demonstrated in our previous studies [23,28].

There are several limitations to our work. First, the time between the first scan and the second scan was 24 h. Although systemic errors would not affect reproducibility, factors that affect FLT kinetics and cancer cell growth could have randomly changed over the 24 h and altered FLT uptake by tumors. Second, we did not measure serum thymidine. The correction of parameters by the use of serum thymidine levels may increase the reproducibility of FLT PET studies [30]. Lastly, the absorbed dose in a tumor exposed to 7.5 MBq of FLT may be as high as 500 mGy [35]. Thus, potential perturbation in cellular proliferation could have occurred in our studies, especially in A431 tumors that had high FLT uptake.

5. Conclusion

Our study on the test–retest reproducibility of the kinetic analysis of FLT PET in mouse tumor models shows that the measurement of macrokinetic parameters is reproducible (standard deviation of ≤20%) in tumors that have a high phosphorylation of FLT. Our study indicates that serial dynamic studies can detect changes in FLT metabolism following anticancer therapy in mouse tumor models.

Acknowledgments

This study was supported by the Real Time Molecular Imaging Research Program of the Korean Science and Engineering Foundation, which is funded by the Ministry of Education, Science and Technology, Republic of Korea, and by the Korea Health 21 R&D Project, Ministry of Health, Welfare and Family Affairs, Republic of Korea (grant no. A062254).

References

[1] Therasse P, Arbuck SG, Eisenhauer EA, Wanders J, Kaplan RS, Rubinstein L, et al. New guidelines to evaluate the response to treatment in solid tumors. J Natl Cancer Inst 2000;92:205–16.
[2] Twombly R. Criticism of tumor response criteria raises trial design questions. J Natl Cancer Inst 2006;98:232–4.
[3] Goffin J, Baral S, Tu D, Nomikos D, Seymour L. Objective responses in patients with malignant melanoma or renal cell cancer in clinical studies do not predict regulatory approval. Clin Cancer Res 2005;11:5928–34.
[4] Canellos GP. Residual mass in lymphoma may not be residual disease. J Clin Oncol 1988;6:931–3.
[5] Colozza M, Azambuja E, Cardoso F, Sotiriou C, Larsimont D, Piccart MJ. Proliferative markers as prognostic and predictive tools in early breast cancer: where are we now? Ann Oncol 2005;16:1723–39.
[6] Shields AF, Grierson JR, Dohmen BM, Machulla HJ, Stayanoff JC, Lawhorn-Crews JM, et al. Imaging proliferation in vivo with [F-18] FLT and positron emission tomography. Nat Med 1998;4:1334–6.
[7] Barthel H, Cleij MC, Collingridge DR, Hutchinson OC, Osman S, He Q, et al. 3′-Deoxy-3′-[^{18}F]fluorothymidine as a new marker for monitoring tumor response to antiproliferative therapy in vivo with positron emission tomography. Cancer Res 2003;63:3791–8.
[8] Oyama N, Ponde DE, Dence C, Kim J, Tai YC, Welch M. Monitoring of therapy in androgen-dependent prostate tumor model by measuring tumor proliferation. J Nucl Med 2004;45:519–25.
[9] Waldherr C, Mellinghoff IK, Tran C, Halpern BS, Rozenqurt N, Safaei A, et al. Monitoring antiproliferative responses to kinase inhibitor therapy in mice with 3′-deoxy-3′-^{18}F-fluorothymidine PET. J Nucl Med 2005;46:114–20.
[10] Leyton J, Latigo JR, Perumal M, Dhaliwal H, He Q, Aboagye EO. Early detection of tumor response to chemotherapy by 3′-deoxy-3′-[^{18}F]-fluorothymidine positron emission tomography: the effect of cisplatin on a fibrosarcoma tumor model in vivo. Cancer Res 2005;65:4202–10.
[11] Pio BS, Park CK, Pietras R, Hsueh WA, Satyamurthy N, Pegram MD, et al. Usefulness of 3′-[F-18]fluoro-3′-deoxythymidine with positron emission tomography in predicting breast cancer response to therapy. Mol Imaging Biol 2006;8:36–42.
[12] Wieder HA, Geinitz H, Rosenberg R, Lordick F, Becker K, Stahl A, et al. PET imaging with [^{18}F]3′-deoxy-3′-fluorothymidine for prediction of response to neoadjuvant treatment in patients with rectal cancer. Eur J Nucl Med Mol Imaging 2007;34:878–83.
[13] Kenny L, Coombes RC, Vigushin DM, Al-Nahhas A, Shousha S, Aboagye EO. Imaging early changes in proliferation at 1 week post chemotherapy: a pilot study in breast cancer patients with 3′-deoxy-3′-[^{18}F]-fluorothymidine positron emission tomography. Eur J Nucl Med Mol Imaging 2007;34:1339–47.
[14] Buck AK, Kratochwil C, Glatting G, Juweid M, Bommer M, Tepsic D, et al. Early assessment of therapy response in malignant lymphoma with the thymidine analogue [^{18}F]FLT. Eur J Nucl Med Mol Imaging 2007;34:1775–82.
[15] Herrmann K, Wieder HA, Buck AK, Schöffel M, Krause BJ, Fend F, et al. Early response assessment using 3′-deoxy-3′-[^{18}F]-fluorothymidine positron emission tomography in high-grade non-Hodgkin's lymphoma. Clin Cancer Res 2007;13:3552–8.
[16] Dittmann H, Dohmen BM, Kehlbach R, Bartusek G, Pritzkow M, Sarbia M, et al. Early changes in [^{18}F]FLT uptake after chemotherapy: an experimental study. Eur J Nucl Med Mol Imaging 2002;29:1462–9.
[17] Perumal M, Pillai RG, Barthel H, Leyton J, Latigo JR, Forster M. Redistribution of nucleoside transporters to the cell membrane provides a novel approach for imaging thymidine synthase inhibition by positron emission tomography. Cancer Res 2006;66:8558–64.
[18] Reske SN, Deisenhofer S. Is 3′-deoxy-3′-[^{18}F]-fluorothymidine a better marker for tumour response than ^{18}F-flurodeoxyglucose? Eur J Nucl Med Mol Imaging 2006;33:S38–43.

[19] Muzi M, Mankoff DA, Grierson JR, Wells JM, Vesselle H, Krohn KA. Kinetic modeling of 3′-deoxy-3′-fluorothymidine in somatic tumors: mathematical studies. J Nucl Med 2005;46:371–80.

[20] Muzi M, Vesselle H, Grierson JR, Mankoff DA, Schmidt RA, Peterson L, et al. Kinetic analysis of 3′-deoxy-3′-fluorothymidine PET studies: validation studies in patients with lung cancer. J Nucl Med 2005;46: 274–82.

[21] Visvikis D, Francis D, Mulligan R, Costa DC, Croasdale I, Luthra SK, et al. Comparison of methodologies for the in vivo assessment of ^{18}FLT utilization in colorectal cancer. Eur J Nucl Med Mol Imaging 2004;31: 169–78.

[22] Shields AF, Briston DA, Chandupatla S, Douglas KA, Lawhorn-Crews J, Collins JM, et al. A simplified analysis of [^{18}F]3′-deoxy-3′-fluorothymidine metabolism and retention. Eur J Nucl Med Mol Imaging 2005;32:1269–75.

[23] Kim SJ, Lee JS, Im KC, Kim SY, Park SA, Lee SJ, et al. Kinetic modeling of 3′-deoxy-3′-^{18}F-fluorothymidine (FLT) for quantitative cell proliferation imaging in subcutaneous mouse tumor models. J Nucl Med 2008;49:2057–66.

[24] Kenny LM, Vigushin DM, Al-Nahhas A, Osman S, Luthra SK, Shousha S, et al. Quantitation of cellular proliferation in tumor and normal tissues of patients with breast cancer by [^{18}F]fluorothymidine-positron emission tomography imaging: evaluation of analytical methods. Cancer Res 2005;65:10104–12.

[25] Kelloff GJ, Krohn KA, Larson SM, Weissleder R, Mankoff DA, Hoffman JM, et al. The progress and promise of molecular imaging probes in oncologic drug development. Clin Cancer Res 2005;11:7967–85.

[26] Tseng JR, Dandekar M, Subbarayan M, Cheng Z, Park JM, Louie S, et al. Reproducibility of 3′-deoxy-3′-^{18}F-fluorothymidine microPET studies in tumor xenografts in mice. J Nucl Med 2005;46:1851–7.

[27] Lee SJ, Oh SJ, Chi DY, Kil HS, Kim EN, Ryu JS, et al. Simple and highly efficient synthesis of 3′-deoxy-3′-[^{18}F]fluorothymidine using nucleophilic fluorination catalyzed by protic solvent. Eur J Nucl Med Mol Imaging 2007;34:1406–9.

[28] Kim JS, Lee JS, Im KC, Kim SJ, Kim SY, Lee DS, et al. Performance measurement of the microPET focus 120 scanner. J Nucl Med 2007;48: 1527–35.

[29] Dandekar M, Tseng JR, Gambhir SS. Reproducibility of ^{18}F-FDG microPET studies in mouse tumor xenografts. J Nucl Med 2007;48: 602–7.

[30] Minn H, Zasady KR, Quint LE, Wahl RL. Lung cancer: reproducibility of quantitative measurements for evaluating 2-[F-18]-fluoro-2-deoxy-D-glucose uptake at PET. Radiology 1995;196: 167–73.

[31] Weber WA, Ziegler SI, Thödtmann R, Hanauske AR, Schwaiger M. Reproducibility of metabolic measurements in malignant tumors using FDG PET. J Nucl Med 1999;40:1771–7.

[32] Muzi M, Spence AM, O'Sullivan F, Mankoff DA, Wells JM, Grierson JR, et al. Kinetic analysis of 3′-deoxy-3′-fluorothymidine in patients with gliomas. J Nucl Med 2006;47:1612–21.

[33] Schiepers C, Chen W, Dahlbom M, Cloughesy T, Hoh CK, Huang SC. ^{18}F-Fluorothymidine kinetics of malignant brain tumors. Eur J Nucl Med Mol Imaging 2007;34:1003–11.

[34] Grierson JR, Shwartz JL, Muzi M, Jordan R, Krohn KA. Metabolism of 3′-deoxy-3′-[F-18]fluorothymidine in proliferating A549 cells: validations for positron emission tomography. Nucl Med Biol 2004;31: 829–37.

[35] Taschereau R, Chatziioannou AF. Monte Carlo simulations of absorbed dose in a mouse phantom from 18-flurine compounds. Med Phys 2007;34:1026–36.